The Journal of Chemical Physics ARTICLE scitation.org/journal/jcp

Threshold photodissociation dynamics of NO_2 studied by time-resolved cold target recoil ion momentum spectroscopy

Cite as: J. Chem. Phys. 151, 174301 (2019); doi: 10.1063/1.5095430
Submitted: 8 March 2019 • Accepted: 10 October 2019 •
Published Online: 4 November 2019

Xiaoyan Ding,[1,2,3] R. Forbes,[2,3,4] M. Kübel,[1,2,3] Kevin F. Lee,[1,2,3] M. Spanner,[3] A. Yu. Naumov,[1,3] D. M. Villeneuve,[1,2,3] A. Stolow,[2,3,5] P. B. Corkum,[1,2,3] and A. Staudte[1,2,3,a)]

AFFILIATIONS

[1]Joint Attosecond Science Laboratory, National Research Council of Canada and University of Ottawa, 100 Sussex Drive, Ottawa, Ontario K1A 0R6, Canada
[2]Department of Physics, University of Ottawa, Ottawa, Ontario K1N 6N5, Canada
[3]National Research Council Canada, 100 Sussex Dr., Ottawa, Ontario K1A 0R6, Canada
[4]Department of Physics and Astronomy, University College London, Gower Street, London WC1E 6BT, United Kingdom
[5]Department of Chemistry, University of Ottawa, Ottawa, Ontario K1N 6N5, Canada

[a)]**Electronic mail:** andre.staudte@nrc.ca

ABSTRACT

We study the near-threshold photodissociation dynamics of NO_2 by a kinematically complete femtosecond pump-probe scheme using a cold target recoil ion momentum spectrometer. We excite NO_2 to the optically bright $\tilde{A}^2B_2$ state with a 400 nm pulse and probe the ensuing dynamics via strong field single and double ionization with a 25 fs, 800 nm pulse. The pump spectrum spans the $NO(X^2\Pi) + O(^3P)$ dissociation channel threshold, and therefore, following internal conversion, excited NO_2 is energetically prepared both "above threshold" (dissociating) and "below threshold" (nondissociating). Experimentally, we can clearly discriminate a weak two-photon pump channel from the dominant single-photon data. In the single ionization channel, we observe NO^+ fragments with nonzero momentum at 200 fs delay and an increasing yield of NO^+ fragments with near-zero momentum at 3.0 ps delay. For double ionization events, we observe a time-varying Coulombic kinetic energy release between the NO^+ and O^+ fragments impulsively created from the evolving "hot" neutral ground state. Supported by classical trajectory calculations, we assign the decreasing Coulombic kinetic energy release at longer time delays to the increasing average NO–O distances in the ground electronic state during its large amplitude phase space evolution toward free products. The time-resolved kinetic energy release in the double ionization channel probes the large amplitude ground state evolution from a strongly coupled "inner region" to a loosely coupled "outer region" where one O atom is on average much further away from the NO. Both the time evolution of the kinetic energy release and the NO^+ angular distributions support our assignments.

I. INTRODUCTION

The near-threshold photodissociation of $NO_2 + h\nu \rightarrow NO(X^2\Pi) + O(^3P)$ is the classic example of ground state unimolecular reaction dynamics. In NO_2, the conical intersection between its two lowest electronic states greatly perturbs the vibrational structure, and the vibronic level distribution up to the dissociation threshold exhibits chaotic dynamics.[1–4] The rich and complex spectroscopy of NO_2 and its low-lying dissociation threshold make it a prototype molecule for investigating ground state unimolecular decay from both experimental and theoretical points of view.[5–13]

We briefly review the well-known photodissociation dynamics of NO_2. Absorption of a 400 nm photon excites NO_2 to its $\tilde{A}^2B_2$ electronic state (see Fig. 1). Following the initial photoexcitation, the nuclear wavepacket on the excited state surface is predominantly localized in the bending mode. Upon multiple passages through a conical intersection, the molecule returns, via internal conversion, to the $\tilde{X}^2A_1$ ground state on a femtosecond time scale.[14,15] A recent *ab initio* study using new potential energy surfaces[16] showed that internal conversion to the ground state occurs on a 50 fs time scale and that, by 200 fs, the initially coherent large amplitude bending motion in the electronic ground state broadly spreads into other coordinates through an intramolecular vibrational energy redistribution (IVR). Consistent with the many prior studies of NO_2 photodissociation, this study showed that, following the first ~200 fs, the subsequent ground state dynamics can be approximated by an exponential decay. If the photon energy exceeds the dissociation threshold (3.115 eV, 397.95 nm[3]), the NO_2 molecule will eventually dissociate into neutral ground state NO and O fragments.[17] The dissociation process has often been described by statistical or phase space theories of unimolecular decay, where the intramolecular vibrational redistribution is assumed to be "instantaneous" on the time scale of dissociation, leading to expectations of exponential decay of the energized molecule.[8] However, classical trajectory simulations reported the existence of multiple time scales during the ground state dissociation, suggesting that the available phase space is divided into a strongly coupled "inner" and a loosely coupled "outer" region.[18] An intramolecular bottleneck separates these phase space regions, and the rate of flow between these regions is different than that for crossing the loose transition state region, leading to products. However, we are not aware of any experimental test of this proposal. This study aims to provide a new observable that will probe this "loose" large amplitude region of the ground state dynamics.

Prior experimental investigations used energy-resolved techniques to measure the detailed final-state product distributions.[19,20] These were subsequently followed by ultrafast time-resolved studies to investigate the neutral photodissociation dynamics.[21–25] Recently, high harmonic spectroscopy,[14] extreme ultraviolet time-resolved photoelectron spectroscopy,[9] and photoelectron-photoion coincidence (PEPICO) spectroscopy[26] have attempted to access the underlying electronic and nuclear dynamics by mapping the electronic state and structural evolution.

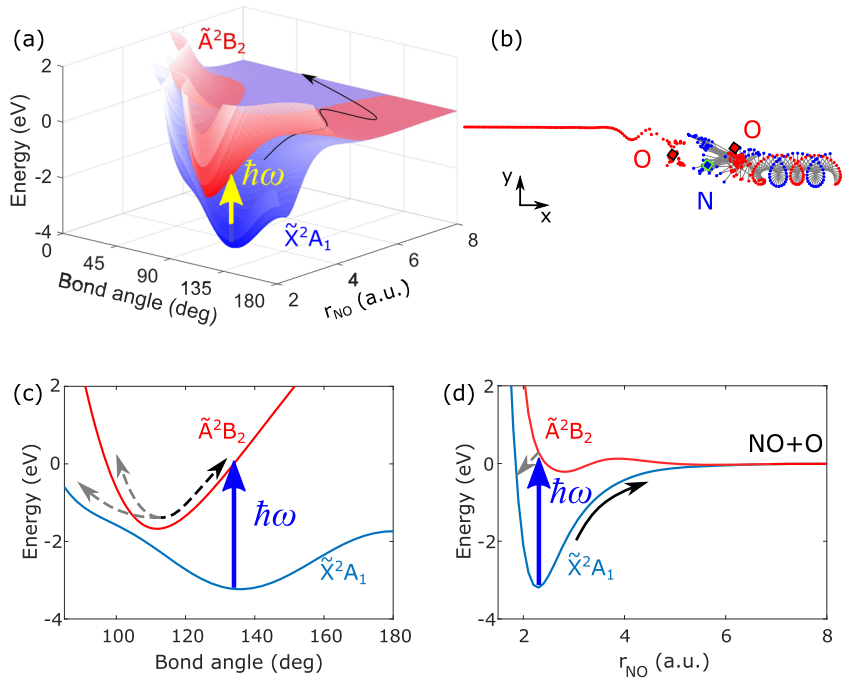

FIG. 1. The near threshold photodissociation dynamics of NO_2. (a) Approximate potential energy surfaces of the ground (blue) and the first excited (red) electronic state of NO_2 as a function of bond angle and one N–O bond length.[35] The other N–O bond length is fixed at 2.26 atomic units (a.u.). In (b), we show an example of a simulated trajectory of NO_2 dissociation on a 2D plane. The blue and red dots show the position of the nitrogen and the two oxygen atoms in the dissociation, respectively. The squares show the initial positions of the atoms. As expected, the "hot" NO_2 molecule undergoes complex motions on the ground state before the NO–O bond significantly stretches along the dissociation coordinate. The molecule eventually dissociates into NO and O, with the NO fragment carrying most of the recoil angular momentum as internal rotation. In (c) and (d), we show one-dimensional cuts through these potential energy surfaces. Single photon absorption can excite the molecule to the $\tilde{A}^2B_2$ state. The wavepacket crosses the conical intersection region several times, shown as dashed arrows in (c). After about 200 fs, the population transfers back to the $\tilde{X}^2A_1$ ground electronic state. When the pump photon energy exceeds the dissociation threshold (3.115 eV), the excited molecule will eventually dissociate on the ground electronic state into free NO + O, indicated by the black arrows in (a) and (d). Importantly, here a strong-field ionization probe is used to directly monitor the evolution of the average NO–O distance in the ground electronic state during the statistical unimolecular decay.

In the time-resolved studies, some ambiguities remain in the interpretation of the data, in part, due to the possible role of multiphoton excitation processes.[17,23,27] An oscillation in the high harmonic signal in the first 200 fs was attributed to electronic dynamics around the conical intersection between $\tilde{A}^2B_2$ and $\tilde{X}^2A_1$ electronic states.[14] Subsequent strong field ionization (SFI) electron ion coincidence experiments highlighted that the form of various experimental observables, which looked oscillatory in nature, were dependent on the pump laser intensity.[26] This indicated that multiphoton pump channels may have been operative in these experiments. Further studies will be required in order to fully discern these apparent discrepancies.

Here, we present a time-resolved strong field ionization study of NO_2 $\tilde{A}^2B_2$–$\tilde{X}^2A_1$ wavepacket dynamics using the 3-dimensional momentum distributions of the fragment ions as observables of the dissociation pathway. We propose a new observable, that of time-resolved Coulomb explosion imaging,[28–32] as an experimental probe of the "statistical" unimolecular evolution of a "hot" ground state toward free products. We argue that this method allows us to probe the unimolecular evolution toward products of an unstable ground state as it samples the longer range region of its available phase space. The NO_2 wavepacket is launched on the $\tilde{A}^2B_2$ state with a weak femtosecond pump pulse centered at 400 nm, thereby energetically spanning both "above threshold" (dissociating) and "below threshold" (nondissociating) states. We probe the ensuing dynamics as a function of time via strong field ionization with a short, intense ($>10^{14}$ W/cm^2) 800 nm laser pulse, which impulsively creates singly and doubly charged ions as well as their associated photoelectrons. These time-dependent ion and electron signals are detected using the kinematically complete Cold Target Recoil Ion Momentum Spectroscopy (COLTRIMS) technique.[33,34] In the $NO^+ + O^+$ double ionization channel, we observe that, at longer pump-probe delays, the kinetic energy release (KER) decreases monotonically with the pump-probe time delay. We argue that this observable is directly related to the evolving average scalar distance (i.e., independent of orientation) between NO and O during ongoing ground state exploration of the available phase space for this "statistical" unimolecular reaction. Supported by rough classical trajectory calculations that motivate this choice of observable, we interpret our results in terms of a phase space evolution from a strongly coupled "inner region," where the three atoms are in close proximity, to an "outer region" where one O atom is on average much further away from the N atom than the other O atom.

II. EXPERIMENTAL SETUP

Experiments using a UV pulse as the pump and strong field ionization as the probe have been used to study several types of molecules.[36–39] In this time-resolved pump-probe experiment, we employ a cold target recoil ion momentum spectrometer. In Fig. 2, we show a schematic diagram of the experimental apparatus. A seeded molecular beam of 5% NO_2 in helium expands through a 30 μm nozzle at a backing pressure of 1 bar. The nozzle is heated to 80 °C to minimize dimer formation. This, combined with the fact that the N_2O_4 has a low absorption cross section at 400 nm,[40] means that the potential effects of N_2O_4 on our results are negligible. We estimate that the NO_2 parallel translational temperature is 105 K in

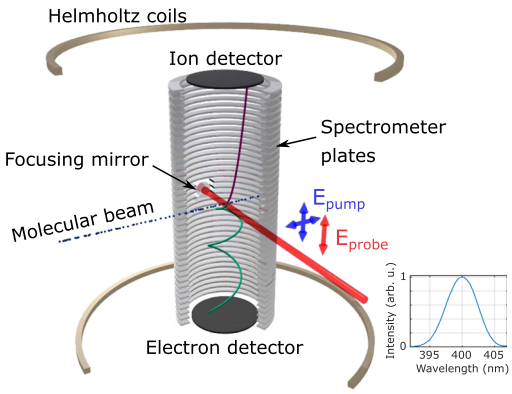

FIG. 2. Sketch of the COLTRIMS spectrometer as well as the laser pump-probe polarization geometries used in the study of the photodissociation dynamics of NO_2. The bottom right inset shows the spectrum of the pump pulse.

the jet propagation direction, based on the measurement of the parent molecule momentum distribution. Our femtosecond Ti:sapphire laser system (Coherent Legend Elite Cryo) delivers 800 nm, 25 fs pulses at a repetition rate of 10 kHz. The output is split into two arms, providing the pump and probe beamlines, respectively. The first arm is frequency doubled using a 300 μm thick Beta Barium Borate (β-BaB_2O_4), BBO, generating the 400 nm pump pulse. The second arm, the probe pulse, remains at the fundamental frequency and is utilized for strong-field ionization. The temporal overlap between the 400 nm pump and 800 nm probe pulses is determined by evaluating nonresonant ionization of H_2. The cross correlation between 800 nm and 400 nm provides an approximate pulse duration of 56 fs for the 400 nm pump pulse. The pump pulse has a center wavelength of 400 nm and 5.5 nm bandwidth at full width half maximum (FWHM). The spectrum of the pump pulse is shown in the bottom right inset of Fig. 2.

The polarization of the probe pulse is parallel to the spectrometer time-of-flight axis. The polarization of the pump pulse is selected to be either parallel or perpendicular to the probe polarization (see Fig. 2). Both pulses are back-focused into the molecular beam with an on-axis 50 mm focal length spherical mirror. By measuring the ion momentum of H_2^+ ionized with a circularly polarized pulse,[41] we establish a pulse energy to intensity scaling. For the results in this paper, we estimate that the Gaussian peak intensity at the laser focus to be 2.4×10^{12} W/cm^2 and 1.2×10^{14} W/cm^2 for the pump and probe pulses, respectively. In the experiment, no ionization events of NO_2 are observed from the pump laser alone. At each polarization geometry, we perform two types of measurements: (i) a scan of the pump-probe delay time from −0.2 ps to +1.0 ps, in steps of 20 fs; (ii) extended acquisition at a few selected time delays in order to significantly reduce statistical noise. The latter measurement permits, for example, the photofragment angular distributions to be extracted at several time delays.

In these experiments, there is a small NO background signal channel that requires subtraction. Assuming NO and NO_2 in the jet have approximately the same strong-field ionization rate, we estimate that there is about 0.03% NO contamination in the NO_2 gas mixture. However, signals from the NO do not depend on the

pump-probe delay. In the following, these events are removed from the data by subtracting an averaged signal at negative delays (−0.2 ps to −0.05 ps), i.e., when the probe precedes the pump. Other time-independent signals, such as dissociative ionization of the ground state NO_2 by the 800 nm probe pulse alone, are also removed by this subtraction method.

III. CALCULATION

In order to simulate the Coulomb explosion probing of the dissociation process on the ground electronic state, we use a simple classical trajectory Monte Carlo method.[18] The classical Hamiltonian for the molecule is written as

$$H = E_R + E_r + E_{bend} + V(R, r, \gamma), \quad (1)$$

where R is the distance between O and the center of mass of NO, r is the NO bond length, and γ is the angle between R and r; $E_R = P_R^2/2m_R$, $E_r = P_r^2/2m_r$, and $E_{bend} = B(R,r)P_\gamma^2$ are the energies corresponding to the NO–O stretch (R), the N–O stretch (r), and the bending mode, respectively; m_R and m_r are the reduced mass of O–NO and NO, respectively. $B(R, r) = 1/(2m_R R^2) + 1/(2m_r r^2)$ is the effective rotational constant of the system. The P's are the momenta in the conjugate coordinates. V (R, r, γ) is an approximate potential energy for NO_2 in its ground electronic state $\tilde{X}^2A_1$. Specifically, we use the analytical potential energy surface from the work of Reignier *et al.*[35] and solve the equations of motion using a 5th order Runge-Kutta method. Although recent theoretical work reported a new and accurate global potential energy surface,[16] we use the potential surface from the work of Reignier *et al.*, as its analytical form allows us to more easily perform the classical trajectory calculations used to motivate our choice of experimental observable. To simulate the experiment, we model the single photon excitation by a 400 nm pulse with a 5 nm bandwidth (FWHM). We choose our Monte Carlo initial conditions as follows: one bond length samples 1.25 ± 0.1 Å, the other bond length samples 1.43 ± 0.1 Å, the bond angle samples 130° ± 15°,[15] and the initial kinetic energy is randomly distributed among E_R, E_r, and E_{bend}. The bond length and bond angle assume uniform distributions within their range. We classically propagate the particles for 3.0 ps. We start with r being the shorter bond length, but at the end of propagation, either r or R can be the dissociation coordinate. We compare the two N–O bond lengths at the end of the propagation in order to decide which bond dissociates. The following results are for the longer dissociation bond.

In Fig. 1(b), we show one example of a simulated, complex dissociation trajectory. For this trajectory, as the NO–O distance increases, the recoiling NO fragment feels a torque due to the asymmetric dissociation geometry and thereby acquires rotational angular momentum. As is well known, the total angular momentum is partitioned between the product NO internal rotation and the photofragment angular recoil distribution. In order to compare with our double ionization experimental results (*vide infra*), we convert the NO–O distance to a Coulomb recoil kinetic energy by assuming that the NO and O fragments are each singly ionized and subsequently interact only via a repulsive Coulomb potential. This allows us to roughly simulate the observed time dependence of the NO^+–O^+ Coulomb explosion energies, the results of which are presented in Sec. IV.

IV. RESULTS AND ANALYSIS

Experimentally, we observe two major channels: a single ionization channel $NO_2 \xrightarrow{pump} (NO_2)^* \xrightarrow{probe} NO^+ + O + e^-$ and a double ionization channel $NO_2 \xrightarrow{pump} (NO_2)^* \xrightarrow{probe} NO^+ + O^+ + 2e^-$. These two channels probe the dynamics of NO_2 dissociation from different perspectives, as discussed in Subsections IV A and IV B.

A. Single ionization probe

We present data associated with the single ionization channel: $NO_2 \xrightarrow{pump} (NO_2)^* \xrightarrow{probe} NO^+ + O + e^-$, where a photoelectron is detected in coincidence with a NO^+ fragment. The momentum of the neutral oxygen atom is obtained via momentum conservation, thus determining the kinetic energy of all three fragments (O, NO^+, e^-).

In Fig. 3(a), we show the kinetic energy release as a function of pump-probe delay. The results associated with the parallel and perpendicular polarizations are qualitatively similar. Hence, for the sake of clarity, only results for the parallel polarization are shown. In Fig. 3(b), we show the kinetic energy release integrated over pump-probe delays from 0.4 ps to 1.0 ps, partitioned into three regions: I, II, and III. We present the time-dependent kinetic energy spectrum for these three regions, 0–0.6 eV (I, blue), 0.6–1.8 eV (II, green), and 1.8–3.5 eV (III, red) in Fig. 3(c). In region I, the signal exhibits a peak at approximately 0.2 ps, then a local minimum at about 0.35 ps, followed by a slow increase to 1.0 ps. Regions II and III maximize at earlier delays and then show a slow, monotonic decrease.

The lowest energy channel, region I, was recently studied using time-resolved Channel-Resolved Above Threshold Ionization (CRATI)[42] by Forbes *et al.*[26] They also observed the peak in the NO^+

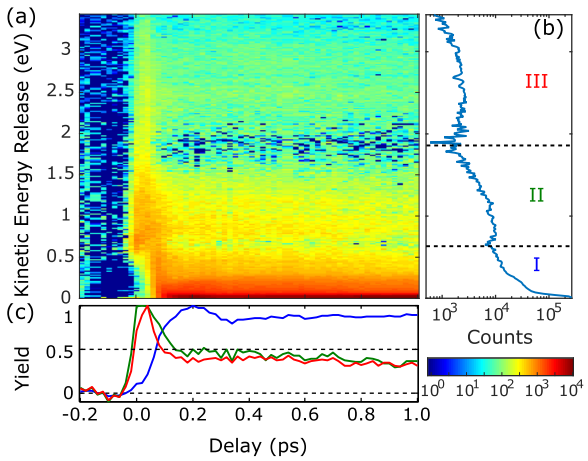

FIG. 3. (a) Time-resolved total kinetic energy release for the channel $NO_2 \rightarrow (NO_2)^* \rightarrow NO^+ + O + e^-$. The background has been subtracted (see main text for details). (b) Kinetic energy release integrated from 0.4 ps to 1 ps. (c) Time-resolved ion yield of NO^+ with different total kinetic energy release: blue curve, region I, 0–0.6 eV; green curve, region II, 0.6–1.8 eV; and red curve, region III, 1.8–3.5 eV.

ion yield at about 200 fs. This peak was explained with an enhanced ionization rate at around a bond angle of 102° from the ground electronic state.[26] Recent theoretical work by Tehlar *et al.*,[16] however, showed that the wavepacket was dispersed in the bending coordinate at about 200 fs. We are also aware that the coordinate dependence of the strong field ionization rates may strongly filter certain ranges of geometries.[26] The discrepancy as to the origin of the peak near 200 fs in NO^+ ion yield may, therefore, require further investigation. At longer pump-probe delays, free, neutral NO recoil fragments appear due to the parent NO_2 unimolecular dissociation on the electronic ground state.

In Fig. 4(a), we show the sum momentum of NO^+ plus the electron in coincidence, along the time-of-flight direction, $p_{z,\mathrm{sum}} = p_{z,\mathrm{e}} + p_{z,\mathrm{NO^+}}$, for the low energy channel (region I). Similar to the temporal behavior of the low energy NO^+ yield [Fig. 3(c), blue curve], we observe peaks around 0.2 ps, followed by a slow increase in this signal at longer delays. At a delay of 200 fs, the sum momentum along the time-of-flight direction exhibits a double peak structure centered around $p_{z,\mathrm{sum}} = 0$ a.u. At longer pump-probe delays, this double peak structure disappears.

This double peak feature is shown more clearly in Fig. 4(b), where the sum momentum distribution is plotted for several specific time delays. Between 0.3 and 1.0 ps, the double peak momentum structure merges into a single peak centered at 0 a.u., with a width of ~6 a.u. (FWHM). The nonzero sum momentum at short pump-probe delays indicates that a third particle must be involved in the $NO^+ + e^-$ channel. As a third charged particle is not detected in these coincidence measurements, we assume that the missing third particle is the neutral oxygen atom in the process $NO_2 \rightarrow NO^+ + O + e^-$. The recoil from the oxygen atom provides the nonzero momentum to the NO^+ fragment. The double-peak structure in the momentum at early pump-probe delays is consistent with dissociative ionization of the excited parent NO_2 with small N–O bond lengths. Several hundred femtoseconds following the pump step, the neutral "hot" ground state molecule evolves toward separated neutral NO and O products. Thus, the recoiling neutral fragments become sufficiently distant that the $NO^+ + e^-$ sum momentum can no longer be affected by the O atom, and therefore, the double-peak is replaced by the single peak centered at zero momentum in Fig. 4(b).

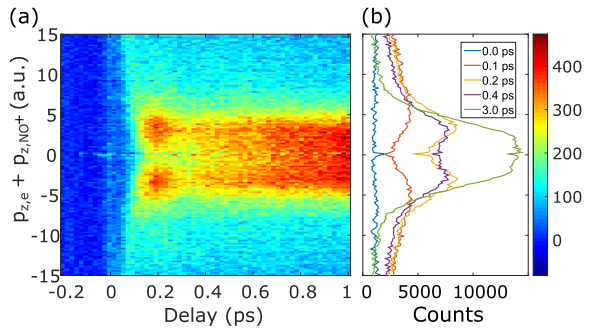

FIG. 4. (a) Sum momentum of $NO^+ + e^-$ in coincidence. (b) Sum momentum distribution for individual delays. As the delay increases, the number of fragments with near-zero momentum increases, indicating an increasing number of NO fragments produced via neutral dissociation.

Since our excitation pulse has a significant fraction of the spectrum with photon energies below the dissociation threshold, many of the optically excited NO_2 molecules will evolve into highly excited rovibrational levels, just below the dissociation threshold, on the ground electronic state. These are unable to dissociate into free NO + O photoproducts. Thus, at long pump-probe delays where large amplitude motions are expected, the strong-field single ionization probe has not yet been demonstrated to distinguish the evolving ensemble of quasibound but eventually dissociating molecules from the bound but highly excited molecules, as both will sample very similar configurations (phase space volumes) on the ground potential energy surface. In Sec. IV B, we discuss the probing of these dissociating (i.e., asymptotically unbound) NO_2 molecules via the double ionization channel.

Highly excited but bound NO_2 molecule sampling large NO–O distances potentially provides a simple experimental measure of time scales associated with an intramolecular vibrational redistribution. In Fig. 5, we plot the yield of events having small sum momenta for NO^+ and e^-. If we associate this growth with phase space evolution toward configurations sampling very long NO–O distances, then this may serve as a proxy for the time scale of intramolecular vibrational redistribution evolving from the strongly coupled "inner region" to a more loosely coupled "outer region," as discussed in the Introduction. To investigate this speculation, we fit the experimental data in Fig. 5 to the growth curve

$$n = n_0[1 - \exp(-t/\tau)], \tag{2}$$

where n is the population of NO_2 with long bond lengths, n_0 is the population of excited NO_2, t is the pump-probe delay, and τ is the effective time constant. The two datasets result in a time constant of 0.65 ± 0.05 ps. In comparison, we estimate the average time constant for product appearance at room temperature to be about 4.18 ps by convoluting the known set of threshold NO + O scattering resonances with our laser pump pulse spectrum.[21] The fitted

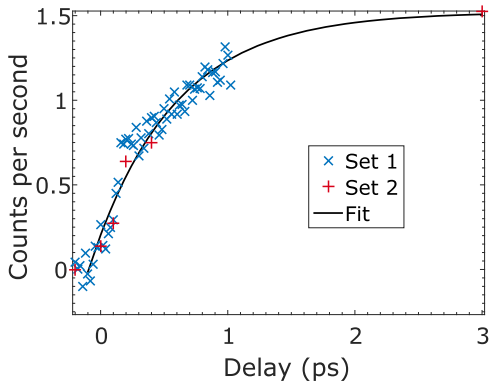

FIG. 5. Events with low sum momentum ($|p_{z,\mathrm{sum}}| < 0.5$ a.u.). Blue cross and red plus signs show two experimental datasets. Set 1 measures from −0.2 ps to 1.0 ps, in steps of 0.02 ps. Set 2 measures at a few specific delays, as is shown in the plot, with longer data acquisition time at each delay. The two datasets are scaled to the same data acquisition time, 1 s (or 10 000 laser shots). The solid black curve is an overall fitting result for the two sets of experimental data using a weighted least squares fitting method.

time constant is much shorter than the average time scale associated with free photoproducts' appearance. This intriguing result may relate to the time scale for transition from an "inner" strongly coupled region of intramolecular vibrational redistribution to a looser "transition state region" involving very large amplitude motions. We believe that high quality trajectory studies on an accurate ground state potential energy surface will be required in order to confirm this speculation.

We now consider the angular dependence of photoexcitation and strong-field ionization. In Fig. 6, we plot the angular distribution of the NO^+ recoil momentum in the laboratory frame. The pump and probe polarizations are parallel for Figs. 6(a) and 6(b) and perpendicular for Figs. 6(c) and 6(d), respectively, as indicated on the left-hand side of the figures. In Figs. 6(a) and 6(c), we show the angular distribution of the NO^+ fragments with the lowest kinetic energy release (KER < 0.06 eV, or $|p_{z,\mathrm{sum}}| < 9$ a.u.). At short pump-probe delays (<400 fs), we observe distinct anisotropic features: a two-lobe structure primarily along the polarization direction for the parallel case and a four-lobe structure for the perpendicular case. As the delay increases, these features become less distinct. By 3.0 ps delay, these two-lobe and four-lobe structures are no longer observable.

The 400 nm pump pulse selectively excites ground state NO_2 molecules whose O–O axis (the molecular y-axis) is aligned along the laser polarization. The strong field ionization of this initially aligned excited state ensemble is the origin of the emission patterns of NO^+ at short pump-probe delays (<400 fs). Disappearance of these features indicates that the initial alignment of the NO_2 molecule is lost over time. We estimate that the rotational wavepacket of NO_2 at a temperature of 50 K dephases in about 1 ps. In our experiments, the NO_2 translational temperature is 105 K and the rotational temperature is generally even higher,[43,44] which means that the dephasing time is shorter. Although the rotation of the molecule becomes slower as the NO–O distance increases, strong mixing of the bending and stretching vibrations during the evolution toward dissociation products is most likely to cause the observed loss of anisotropy.

In Figs. 6(b) and 6(d), we show the NO^+ angular distributions for the higher kinetic energy (0.6 < KER < 1.8 eV) channel for parallel and perpendicular polarizations, respectively. The much higher anisotropy in this channel, together with the higher kinetic energy release, indicates that this channel is likely due to the absorption of two 400 nm pump photons.

The absorption of two 400 nm photons would project the ground state molecules onto the $(2)^2B_2$ state, which is known to have several channels open to dissociation.[17] The dissociation along the $(2)^2B_2$ surface can occur promptly and produce fragments with a kinetic energy release of up to 3.1 eV. Dissociation along the $(4)^2A'$ and $(5)^2A'$ surfaces would produce fragments with a kinetic energy release of up to 1.1 eV. The short time behavior (within 100 fs) of the NO^+ yield is also consistent with this interpretation: the fast initial rise of the NO^+ yield is due to the increased ionization rate (decreased ionization potential) of the $(2)^2B_2$ state. The prompt dissociation leads to the observed rapid decay in this channel. This

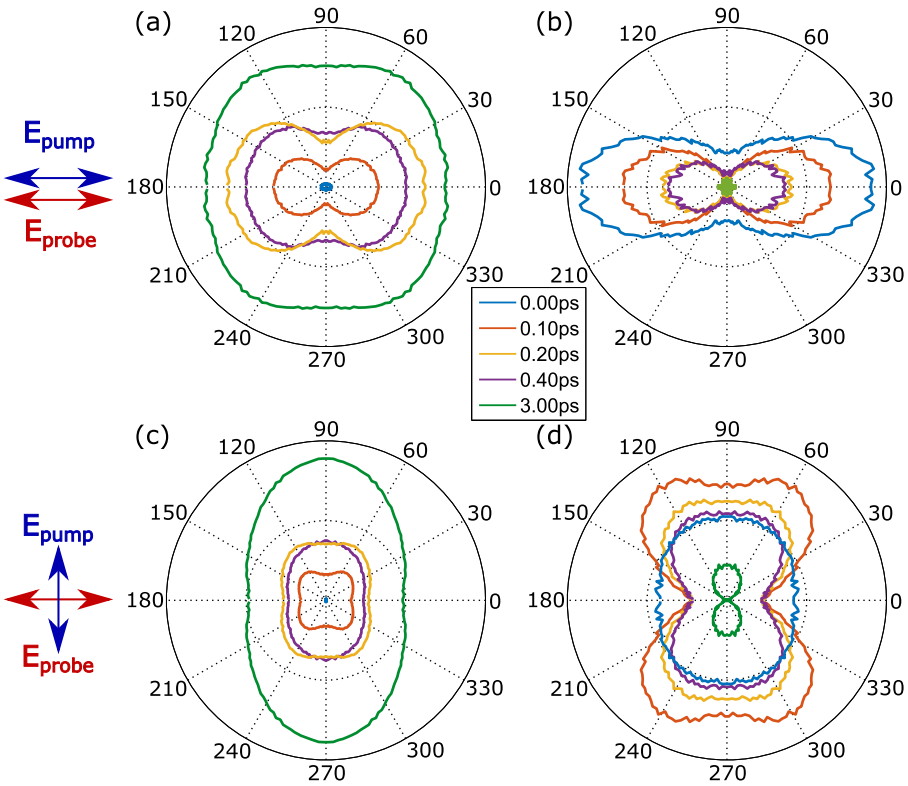

FIG. 6. NO^+ angular distribution in the lab frame with low kinetic energy release 0.0–0.06 eV [(a) and (c)] and the higher kinetic energy range (0.6–1.8 eV) [(b) and (d)], respectively. The radial coordinate shows the ion yield as a function of recoil angle. The left insets show the laser polarizations relative to the angles in the plots.

result and its discussion are consistent with and supported by the prior analysis of two-photon pump absorption with CRATI probing by Forbes *et al.*[26]

For the parallel pump and probe polarization geometry, shown in Fig. 6(b), the NO^+ angular distributions remain qualitatively similar up to at least 400 fs after excitation: the anisotropy is not lost at longer time delays, as it is for the low energy channel shown in Fig. 6(a). The NO^+ fragments are emitted preferentially along the polarization direction. In order to identify whether this anisotropic NO^+ emission is caused by the pump or the probe pulse, we turn to the perpendicular polarization geometry. In Fig. 6(d), we show that the anisotropy follows the pump polarization direction for time delays of up to 3.0 ps, which confirms that the pump process dominantly contributes to the anisotropy.

We remark on a qualitatively striking difference between the low energy [Figs. 6(a) and 6(c)] and high energy [Figs. 6(b) and 6(d)] NO^+ channels: whereas in the low energy channel, the NO^+ yield increases with the pump-probe delay, the yield in the high energy channel converges toward zero by 3.0 ps. In a prompt photodissociation process, most of the free NO and O fragments would appear shortly after the excitation pulse. Thus, after a few hundred femtoseconds, the number of free neutral NO fragments in the interaction region can be expected to remain constant. Therefore, the NO^+ yield should not depend on the pump-probe delay after an initial change. In contrast, we observe a steady decrease of high energy NO^+ after 200 fs.

In summary, the high kinetic energy channels of NO_2 single ionization exhibit a short term time-dependent ion yield and a time-dependent angular fragmentation that is consistent with a two-photon excitation of NO_2 to the $(2)^2B_2$ state. However, further investigation is required in order to explain the decreasing yield of this channel at long time delays.

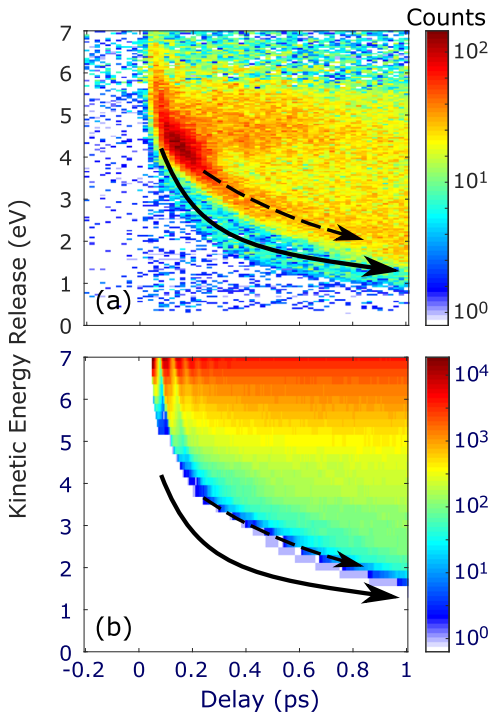

FIG. 7. (a) Experimental and (b) classical trajectory calculations of the Coulombic kinetic energy release for NO^+ and O^+. (b) includes 6.5×10^4 trajectories, and each vertical slice is a histogram of the trajectories at the corresponding delay. Dashed and solid arrows in (a) show single and multiphoton dissociation. These arrows are reproduced in (b), showing good agreement between calculation and experiment for the single photon dissociation events (dashed arrow). The calculation assumes single photon excitation by the 400 nm pump. For further discussion, see main text.

B. Double ionization probe

In the following, we present our results where the probe laser doubly ionizes the excited NO_2 molecule. The photofragmentation dynamics of doubly charged ions can be complex. However, as the average NO–O bond distance increases during the dissociation, the short range (non-Coulombic) interactions will fall off more quickly with internuclear separation than the long-range repulsive Coulomb potential. This suggests that the Coulomb repulsion limit may be achieved for dissociating NO_2 molecules with large NO–O bond distances. In this limit, we can use the kinetic energy release in the doubly ionized channel as a measure of the average distance between the neutral NO and O as a function of time. This measurement, we propose, is related to the propensity for phase space evolution to sample increasing NO–O distances as a function of time. This suggestion is explored in more detail below.

In Fig. 7(a), we show the total ion kinetic energy release for the double ionization channel $NO_2 \xrightarrow{\text{pump}} (NO_2)^* \xrightarrow{\text{probe}} NO^+ + O^+ + 2e^-$. We observe a clear contour of decreasing kinetic energy, marked by the dashed arrow. By comparing with the single photon calculations of Fig. 7(b), we assign this channel to single photon dissociation. Interestingly, in the experiment, we observe a broad and long-lived kinetic energy distribution in the area above the dashed arrow, shown in Fig. 7(a). This broad distribution suggests strong field ionization of a broad range of NO–O distances in the "hot" ground state. We anticipate that this broad range will contain double ionization signals from both the "above threshold" and the "below threshold" channels discussed above. As the pump-probe delay increases, the "above threshold" events will continually proceed toward dissociation and thus lower kinetic energy release. The "below threshold" events, on the other hand, will remain in the broad range since they do not dissociate. Additionally, we observe a much weaker dissociation channel, marked by the solid arrow. We note that the kinetic energy release in this latter channel decreases much faster with the pump-probe time delay than the dominant one-photon channel (dashed arrow). Furthermore, the calculation of the one-photon excitation in Fig. 7(b) shows no intensity along the solid arrow. These two aspects suggest a prompt dissociation process due to a multiphoton pump process.

We roughly simulate the dissociation of neutral NO_2 on its ground electronic state using classical trajectory methods described in Sec. III. Assuming that, at long distances, the interaction between NO^+ and O^+ is purely Coulombic, we obtain the kinetic energy release as being inversely proportional to the scalar distance R_{NO-O}. The results of this calculation are shown in Fig. 7(b). Although the NO^+–O^+ interaction is non-Coulombic at short NO–O distances,

this approximation becomes increasingly justified as the NO–O distance increases. Comparing Figs. 7(a) and 7(b), we observe that the kinetic energy release of most events seen in the experimental data is in the same range as in the calculation. This supports the argument that the events in Fig. 7(a) both on and above the dashed arrow are due to a single 400 nm photon absorption, whereas the prompt channel, marked by the solid arrow, is not captured by our single pump photon calculation. Therefore, this latter channel is assigned to the absorption of two 400 nm pump photons. We observe in Fig. 7(a) that the double ionization signal is the strongest along the dashed arrow. We suggest that this is both consistent with and expected by the preferential enhanced ionization[45] of longer NO–O distances by the probe pulse.

As discussed above, our pump pulse prepares both "above threshold" and "below threshold" highly excited NO_2 molecules in their ground electronic state. The data and calculations shown in Fig. 7 suggest that we can distinguish these two cases by their time-resolved kinetic energy release. We now consider the photofragment angular distribution as a function of pump-probe delay. We expect that more rapidly dissociating molecules will quickly increase their NO–O bond length and, due to the larger interfragment distance, have a reduced kinetic energy release in Coulomb explosion. In contrast, more slowly dissociating molecules will retain a shorter NO–O distance as a function of time and, concomitantly, produce a relatively high kinetic energy release. In Figs. 8(a) and 8(c), we show the angular distributions for relatively quickly dissociating molecules (KER < 2.0 eV) at 3.0 ps delay, using parallel and perpendicular laser polarization geometries. In Figs. 8(b) and 8(d), we show the angular distributions for the slower dissociation (3.5 eV < KER < 5.5 eV) for parallel and perpendicular polarization geometries, respectively.

For the low energy fragments [Figs. 8(a) and 8(c)], at 3.00 ps delay, dominated by the channel along the dashed arrow, we see that most NO^+–O^+ recoil events are preferentially aligned along the pump laser polarization direction. The fitted β_2 parameter for Fig. 8(a) is 0.54 ± 0.04. This must be compared to the state-resolved photofragment imaging results of Softley and co-workers.[46] They determined that the average β_2 varies strongly with excess energy above threshold in the following ranges: for 0–100 cm^{-1}, $\beta_2 \sim 0.5$; for 100–200 cm^{-1}, β_2 fluctuates; and for 200–300 cm^{-1}, $\beta_2 \sim 0.75$. Thus, the state and energy averaged β_2 parameter in the fit to Fig. 8(a) (which is at 3.0 ps delay, after the majority of neutral ground state dissociation events are completed) agrees with the prior state resolved studies. This further supports our assignment that the dissociation events along the dashed line in Fig. 7 are indeed due to the one-photon dissociation of the "above threshold" ground state NO_2 molecules. Furthermore, the photofragment angular distribution in the low energy region agrees with our classical trajectory calculation results, the black curve in Fig. 8(a). In this calculation, we (artificially) align the initial O–O axis of the initial ground state NO_2 molecules to be only parallel to the pump laser polarization. The trajectory calculations do not consider the pump polarization. The alignment shown here is a limiting case wherein we assume that the pump polarization is exactly along the initial O–O axis. The angle shown in Fig. 8 is the angle between the final NO–O bond and the direction of the initial O–O axis. As expected, the

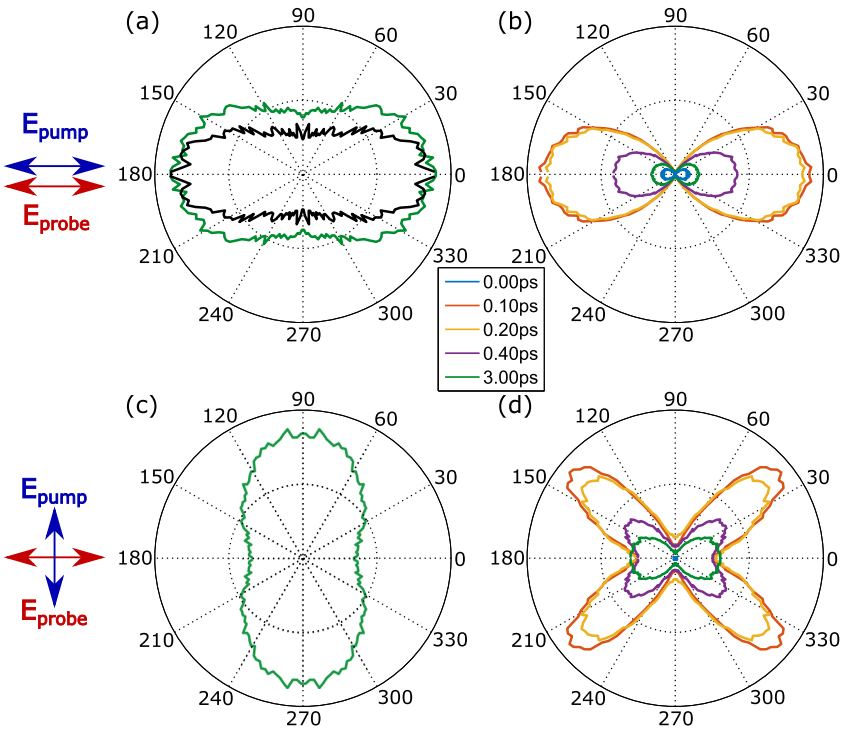

FIG. 8. Angular distribution of NO^+–O^+ with a low kinetic energy (KER < 2 eV) at 3.0 ps time delay [(a) and (c)] and high kinetic energy release (3.5 < KER < 5.5 eV) as a function of time delay [(b) and (d)], respectively. The corresponding pump and probe laser polarizations are shown on the left. The black curve is the simulated photofragment angular distribution for NO + O dissociation, with the initial O–O axis parallel to the pump laser polarization axis.

calculation result is more anisotropic than experimental data, due to the lack of averaging over the initial neutral ground state axis distribution. Nevertheless, the calculation is consistent with our experimental results and those from the prior studies, further supporting our assignment.

We now discuss the Coulomb explosion detection of events in the higher energy region of Fig. 7. These events are interpreted as being due to the Coulomb explosion of "below threshold" and quasibound but not yet dissociated NO_2 molecules in the ground electronic state. At short pump-probe delays, we expect that most excited molecules have their O–O axis preferentially aligned with the pump pulse, due to the y-polarized (C_{2v} symmetry) transition dipole associated with the one-photon excitation process. This leads to a NO–O axis distribution, which is primarily aligned along the pump pulse polarization. However, enhanced ionization of a dissociating molecule is often strongly enhanced when the molecular and laser polarization axes coincide.[47] Therefore, a strong influence of the probe pulse polarization on the observed fragmentation angular distribution can be expected. Indeed, Figs. 8(b) and 8(d) reveal a very different dependence of the angular distribution on the pump-probe polarization geometry for short pump-probe delays. Similar to the single ionization results of Fig. 6, the double ionization photofragment angular distributions of Fig. 8 also show two- and four-lobe structure for the parallel and perpendicular polarization geometries, respectively. However, in contrast to the single ionization, the modulation depth in the angular distributions of the double ionization channel is close to unity. As the time delay increases, the difference between the results from the two polarization situations decreases: both end up with very similar two-lobe distributions, indicating the loss of the alignment. Two effects contribute to the disappearance of the alignment: the strong rovibrational redistribution (where bending leads to a loss of the correlation between the laser polarization and the fragment emission directions) and the slower overall rotation of the molecular frame. These two effects are coupled and cannot be separated in our results.

V. CONCLUSION

We study NO_2 photodissociation at 400 nm excitation and probe the ground state unimolecular dynamics as a function of pump-probe time delay using single and double strong field ionization in a COLTRIMS apparatus. We observe a low energy channel and two high energy channels in the single ionization case. The low energy channel is assigned to single photon excitation and comprises both single ionization of threshold dissociation channels and dissociative ionization of highly vibrationally excited but bound parent molecules. Our results are consistent with the assumption that the intramolecular vibrational redistribution occurs on a much shorter time scale than the photodissociation. The single photon dissociation channel is more clearly distinguished in the double ionization case, where the NO–O distance appears to be directly mapped onto the Coulombic repulsion kinetic energy release. In the double ionization case, we observe both prompt and delayed dissociation processes. Consistent with our calculation, the most observed events are due to single photon pump excitation. The small, prompt dissociation channel involves more than one pump photon. The photofragment angular distributions are also consistent with a statistical unimolecular decay, with the correlation between the recoil direction and the laser polarization direction vanishing at long pump-probe delays.

In our view, a most intriguing aspect of these experiments is the observation that, in the double ionization channel, the $NO^+ + O^+$ Coulombic recoil kinetic energy decreases with the time delay. This must be related to the average increase in the NO–O distance as the excited system explores the ground state phase space on its way to separated products. The Coulomb explosion kinetic energy release varies inversely with the distance between fragments. We suggest that this measure is a unique probe of the average NO–O distance during the statistical unimolecular decay of NO_2. In fact, we are not aware of any other observable that directly probes the evolution of the average distance between fragments during a statistical decay. By combining these COLTRIMS results with high accuracy ground state classical trajectory studies, one could verify this intriguing suggestion. In order to probe the full 3D molecular geometry during ground state fragmentation, one will need ionization to higher charge states, thus approaching the three-body Coulomb explosion limit. Such experiments would benefit from intense few-cycle, circularly polarized pulses at a high repetition rate, reducing the alignment dependent ionization bias and improving statistics.

ACKNOWLEDGMENTS

We thank A. Avery and D. Crane for technical support. R. Forbes is grateful to the Engineering and Physical Sciences Research Council (EPSRC) for a research studentship. We acknowledge funding from CFI, ORF, NSERC, and NRC. This project was supported by the Joint Centre for Extreme Photonics, and has received funding from the European Union's Framework Programme for Research and Innovation Horizon 2020 (2014-2020) under the Marie Skłodowska-Curie Grant Agreement No. 657544.

REFERENCES

[1] A. Delon, R. Jost, and M. Lombardi, "NO_2 jet cooled visible excitation spectrum: Vibronic chaos induced by the $\tilde{X}^2A_1$-$\tilde{A}^2B_2$ interaction," J. Chem. Phys. **95**, 5701–5718 (1991).

[2] A. Delon, R. Jost, and M. Jacon, "Laser induced dispersed fluorescence spectroscopy of 107 vibronic levels of NO_2 ranging from 12000 to 17600 cm^{-1}," J. Chem. Phys. **114**, 331–344 (2001).

[3] R. Jost, J. Nygård, A. Pasinski, and A. Delon, "The photodissociation threshold of NO_2: Precise determination of its energy and density of states," J. Chem. Phys. **105**, 1287–1290 (1996).

[4] R. Georges, A. Delon, and R. Jost, "The visible excitation spectrum of jet cooled NO_2: The chaotic behavior of a set of $^2B_2$ vibronic levels," J. Chem. Phys. **103**, 1732–1747 (1995).

[5] T. J. Butenhoff and E. A. Rohlfing, "Laserinduced gratings in free jets. I. Spectroscopy of predissociating NO_2," J. Chem. Phys. **98**, 5460 (1993).

[6] D. Stolyarov, E. Polyakova, I. Bezel, and C. Wittig, "Rate coefficients for photoinitiated NO_2 unimolecular decomposition: Energy dependence in the threshold regime," Chem. Phys. Lett. **358**, 71–76 (2002).

[7] R. Jost, G. Michalski, and M. Thiemens, "Comparison of rovibronic density of asymmetric versus symmetric NO_2 isotopologues at dissociation threshold: Broken symmetry effects," J. Chem. Phys. **123**, 054320 (2005).

[8] P. Dupré, "Photodissociation resonances of jet-cooled NO_2 at the dissociation threshold by CW-CRDS," J. Chem. Phys. **142**, 174305 (2015).

[9] A. von Conta, A. Tehlar, A. Schletter, Y. Arasaki, K. Takatsuka, and H. Wörner, "Conical-intersection dynamics and ground-state chemistry probed by extreme-ultraviolet time-resolved photoelectron spectroscopy," Nat. Commun. **9**, 3162 (2018).

[10]S. Grebenshchikov, H. Flothmann, R. Schinke, I. Bezel, C. Wittig, and S. Kato, "K_α-mixing in the unimolecular dissociation of NO_2 studied by classical dynamics calculations," Chem. Phys. Lett. **285**, 410–416 (1998).
[11]D. M. Hirst, "*Ab initio* potential energy surfaces for excited states of the NO_2^+ molecular ion and for the reaction of N^+ with O_2," J. Chem. Phys. **115**, 9320 (2001).
[12]A. T. J. B. Eppink, B. J. Whitaker, E. Gloaguen, B. Soep, A. M. Coroiu, and D. H. Parker, "Dissociative multiphoton ionization of NO_2 studied by time-resolved imaging," J. Chem. Phys. **121**, 7776 (2004).
[13]Y. Arasaki, K. Wang, V. McKoy, and K. Takatsuka, "Monitoring the effect of a control pulse on a conical intersection by time-resolved photoelectron spectroscopy," Phys. Chem. Chem. Phys. **13**, 8681–8689 (2011).
[14]H. J. Wörner, J. B. Bertrand, B. Fabre, J. Higuet, H. Ruf, A. Dubrouil, S. Patchkovskii, M. Spanner, Y. Mairesse, V. Blanchet, E. Mével, E. Constant, P. B. Corkum, and D. M. Villeneuve, "Conical intersection dynamics in NO_2 probed by homodyne high-harmonic spectroscopy," Science **334**, 208 (2011).
[15]Y. Arasaki and K. Takatsuka, "Quantum wavepacket dynamics for time-resolved photoelectron spectroscopy of the NO_2 conical intersection," Chem. Phys. **338**, 175–185 (2007).
[16]A. Tehlar, A. von Conta, Y. Arasaki, K. Takatsuka, and H. J. Wörner, "*Ab initio* calculation of femtosecond-time-resolved photoelectron spectra of NO_2 after excitation to the A-band," J. Chem. Phys. **149**, 034307 (2018).
[17]I. Wilkinson and B. J. Whitaker, "Some remarks on the photodynamics of NO_2," Annu. Rep. Prog. Chem., Sect. C: Phys. Chem. **106**, 274–304 (2010).
[18]S. Y. Grebenshchikov, C. B. Flöthman, and R. S. Kato, "Unimolecular dissociation of NO_2. I. Classical trajectory and statistical calculations on a global potential energy surface," J. Chem. Phys. **111**, 619 (1999).
[19]D. Robie, M. Hunter, J. Bates, and H. Reisler, "Product state distributions in the photodissociation of expansion-cooled NO_2 near the NO($X^2\Pi$) $v = 1$ threshold," Chem. Phys. Lett. **193**, 413 (1992).
[20]M. Hunter, S. A. Reid, D. C. Robie, and H. Reisler, "The monoenergetic unimolecular reaction of expansion-cooled NO_2: NO product state distributions at excess energies 0–3000 cm^{-1}," J. Chem. Phys. **99**, 1093 (1993).
[21]S. I. Ionov, G. A. Brucker, C. Jaques, Y. Chen, and C. Wittig, "Probing the $NO_2 \rightarrow NO+O$ transition state via time resolved unimolecular decomposition," J. Chem. Phys. **99**, 3420 (1993).
[22]A. Vredenborg, W. G. Roeterdink, and M. H. M. Janssen, "Femtosecond time-resolved photoelectron-photoion coincidence imaging of multiphoton multichannel photodynamics in NO_2," J. Chem. Phys. **128**, 204311 (2008).
[23]J. B. Hamard, R. Cireasa, B. Chatel, V. Blanchet, and B. J. Whitaker, "Quantum interference in NO_2," J. Phys. Chem. A **114**, 3167 (2010).
[24]I. Bezel, P. Ionov, and C. Wittig, "Photoinitiated unimolecular decomposition of NO_2: Rotational dependence of the dissociation rate," J. Chem. Phys. **111**, 9267 (1999).
[25]N. T. Form, B. J. Whitaker, L. Poisson, and B. Soep, "Time-resolved photoion and photoelectron imaging of NO_2," Phys. Chem. Chem. Phys. **8**, 2925–2932 (2006).
[26]R. Forbes, A. E. Boguslavskiy, I. Wilkinson, J. G. Underwood, and A. Stolow, "Excited state wavepacket dynamics in NO_2 probed by strong-field ionization," J. Chem. Phys. **147**, 054305 (2017).
[27]R. Cireasa, C. M. Jean-Benoît Hamard, and V. Blanchet, "Imaging fast relaxation dynamics of NO_2," Phys. Scr. **80**, 048106 (2009).
[28]F. Légaré, K. F. Lee, A. D. Bandrauk, D. M. Villeneuve, and P. B. Corkum, "Laser Coulomb explosion imaging for probing ultra-fast molecular dynamics," J. Phys. B: At., Mol. Opt. Phys. **39**, S503–S513 (2006).
[29]T. Ergler, A. Rudenko, B. Feuerstein, K. Zrost, C. D. Schröter, R. Moshammer, and J. Ullrich, "Spatiotemporal imaging of ultrafast molecular motion: Collapse and revival of the D_2^+ nuclear wave packet," Phys. Rev. Lett. **97**, 193001 (2006).
[30]X. Zhou, P. Ranitovic, C. W. Hogle, J. H. D. Eland, H. C. Kapteyn, and M. M. Murnane, "Probing and controlling non-Born-Oppenheimer dynamics in highly excited molecular ions," Nat. Phys. **8**, 232–237 (2012).
[31]A. S. Alnaser, B. Ulrich, X. M. Tong, I. V. Litvinyuk, C. M. Maharjan, P. Ranitovic, T. Osipov, R. Ali, S. Ghimire, Z. Chang, C. D. Lin, and C. L. Cocke, "Simultaneous real-time tracking of wave packets evolving on two different potential curves in H_2^+ and D_2^+," Phys. Rev. A **72**, 030702 (2005).
[32]I. A. Bocharova, A. S. Alnaser, U. Thumm, T. N. D. Ray, C. L. Cocke, and I. V. Litvinyuk, "Time-resolved Coulomb-explosion imaging of nuclear wave-packet dynamics induced in diatomic molecules by intense few-cycle laser pulses," Phys. Rev. A **83**, 013417 (2011).
[33]J. Ullrich, R. Moshammer, A. Dorn, R. Dörner, L. P. H. Schmidt, and H. Schmidt-Böcking, "Recoil-ion and electron momentum spectroscopy: Reaction-microscopes," Rep. Prog. Phys. **66**, 1463 (2003).
[34]M. Haertelt, X.-B. Bian, M. Spanner, A. Staudte, and P. B. Corkum, "Probing molecular dynamics by laser-induced backscattering holography," Phys. Rev. Lett. **116**, 133001 (2016).
[35]D. Reignier, T. Stoecklin, P. Halvick, A. Voronin, and J. C. Rayez, "Analytical global potential energy surfaces of the two lowest $^2A'$ states of NO_2," Phys. Chem. Chem. Phys. **3**, 2726 (2001).
[36]M. Burt *et al.*, "Coulomb-explosion imaging of concurrent CH_2BrI photodissociation dynamics," Phys. Rev. A **96**, 043415 (2017).
[37]F. Allum *et al.*, "Coulomb explosion imaging of CH_3I and CH_2ClI photodissociation dynamics," J. Chem. Phys. **149**, 204313 (2018).
[38]W. Li, A. A. Jaroń-Beckera, C. W. Hoglea, V. Sharmaa, X. Zhoua, A. Beckera, H. C. Kapteyna, and M. M. Murnanea, "Visualizing electron rearrangement in space and time during the transition from a molecule to atoms," Proc. Natl. Acad. Sci. U. S. A. **107**, 20219–20222 (2010).
[39]M. Kotur, T. C. Weinacht, C. Zhou, and S. Matsika, "Strong-field molecular ionization from multiple orbitals," Phys. Rev. X **1**, 021010 (2011).
[40]H. K. Roscoe and A. K. Hind, "The equilibrium constant of NO_2 with N_2O_4 and the temperature dependence of the visible spectrum of NO_2: A critical review and the implications for measurements of NO_2 in the polar stratosphere," J. Atmos. Chem. **16**, 257 (1993).
[41]I. V. Litvinyuk, K. F. Lee, P. W. Dooley, D. M. Rayner, D. M. Villeneuve, and P. B. Corkum, "Alignment-dependent strong field ionization of molecules," Phys. Rev. Lett. **90**, 233003 (2003).
[42]A. E. Boguslavskiy, J. Mikosch, A. Gijsbertsen, M. Spanner, S. Patchkovskii, N. Gador, M. J. J. Vrakking, and A. Stolow, "The multielectron ionization dynamics underlying attosecond strong-field spectroscopies," Science **335**, 1336 (2012).
[43]F. J. Aoiz, L. Bañnares, V. J. Herrero, B. Martínez-Haya, M. Menéndez, P. Quintana, I. Tanarro, and E. Verdasco, "Gas phase molecular relaxation at very low temperatures. A comparative study of N_2 and its mixtures with He and Ne," Vacuum **64**, 417–423 (2002).
[44]S. Montero, F. Thibault, G. Tejeda, and J. M. Fernández, "Rotranslational state-to-state rates and spectral representation of inelastic collisions in low-temperature molecular hydrogen," J. Chem. Phys. **125**, 124301 (2006).
[45]E. Constant, H. Stapelfeldt, and P. B. Corkum, "Observation of enhanced ionization of molecular ions in intense laser fields," Phys. Rev. Lett. **76**, 4140–4143 (1996).
[46]S. J. Matthews, S. Willitsch, and T. P. Softley, "Fully state-selected VMI study of the near-threshold photodissociation of NO_2: Variation of the angular anisotropy parameter," Phys. Chem. Chem. Phys. **9**, 5656–5663 (2007).
[47]A. Staudte, D. Pavičić, S. Chelkowski, D. Zeidler, M. Meckel, H. Niikura, M. Schöffler, S. Schössler, B. Ulrich, P. Rajeev, T. Weber, T. Jahnke, D. Villeneuve, A. Bandrauk, C. Cocke, P. Corkum, and R. Dörner, "Attosecond strobing of two-surface population dynamics in dissociating H_2^+," Phys. Rev. Lett. **98**, 073003 (2007).